Journal of Innovative Optical Health Sciences
Vol. 4, No. 4 (2011) 447–462

DOI: 10.1142/S179354581100168X

ENTROPY TOLERANT FUZZY C-MEANS IN MEDICAL IMAGES

S. R. KANNAN[*,§], S. RAMATHILAGAM[†], R. DEVI[*]
and YUEH-MIN HUANG[‡]
[*]*Department of Mathematics*
Ramanujan School of Mathematical Sciences
Pondicherry University, India

[†]*Department of Mathematics*
Periyar Government College, Cuddalore, India

[‡]*Department of Engineering Science*
National Cheng Kung University, Tainan, Taiwan
[§]*srkannan.mat@pondiuni.edu.in*

Accepted 14 June 2011

Segmenting the Dynamic Contrast-Enhanced Breast Magnetic Resonance Images (DCE-BMRI) is an extremely important task to diagnose the disease because it has the highest specificity when acquired with high temporal and spatial resolution and is also corrupted by heavy noise, outliers, and other imaging artifacts. In this paper, we intend to develop efficient robust segmentation algorithms based on fuzzy clustering approach for segmenting the DCE-BMRs. Our proposed segmentation algorithms have been amalgamated with effective kernel-induced distance measure on standard fuzzy c-means algorithm along with the spatial neighborhood information, entropy term, and tolerance vector into a fuzzy clustering structure for segmenting the DCE-BMRI. The significant feature of our proposed algorithms is its capability to find the optimal membership grades and obtain effective cluster centers automatically by minimizing the proposed robust objective functions. Also, this article demonstrates the superiority of the proposed algorithms for segmenting DCE-BMRI in comparison with other recent kernel-based fuzzy c-means techniques. Finally the clustering accuracies of the proposed algorithms are validated by using silhouette method in comparison with existed fuzzy clustering algorithms.

Keywords: Fuzzy clustering; algorithms; entropy method; segmentation; medical images.

1. Introduction

Medical images are a standard tool for identifying a variety of cancers, tumors, and lesions in the medical field. Particularly, breast cancer is a leading cancer causing women mortality. Identifying the early stage of cancer is essential in controlling the mortality rate. At the initial stage, X-ray imaging is used to obtain information about the breast cancer without surgery. In recent years, Magnetic Resonance Imaging technique has been used to find the anatomic structure of breast cancer, because it is non-invasive and it has more contrast between the tissues. More recently, to differentiate similar signal behaviors, the dynamic contrast-enhanced MRI

(DCE-MRI) is used effectively. Further, the DCE-MRI of the breast is an important imaging technique for early breast cancer detection.[1] Though DCE-MRI[2,3] is used in clinical practice for diagnosing diseases, it has considerable limitations. The images are highly affected because of breathing of patient, intensity inhomogeneities, partial volume effect, and other noises. So it is very important to segment[4–7] the images before it goes for diagnosing the breast-related diseases. Initially, medical images have been segmented manually, but the manual segmentation consumes more time, and sometimes human errors occurred during segmentation. So researchers have introduced mathematics-assisted automated segmentation methods for segmenting the breast medical images.

This paper tries to develop clustering-based segmentation method for segmenting medical images. Cluster analysis is the organization of a collection of elements into clusters based on similarity. The data elements within a cluster are more related than the data elements in the other clusters. The hard[8] partitioning controls every data element in the dataset to precisely one cluster, but fuzzy partitioning permits each data element to all the clusters with different meaningful membership degrees. It formulates the fuzzy clustering segmentation technique to be capable of preserving more information from the original image than the hard segmentation technique. Further, the fuzzy clustering approach of segmentation algorithm[9,10] without necessitating any prior information, and segmentation is done with the information extorted from the image itself. In recent years, Fuzzy c-Means (FCM) algorithm has gained much attention for segmenting medical images by various researchers in the field of image segmentation.[11,12] Even though the conventional FCM algorithm works well in spherical clusters, it suffers because of Euclidean distance. FCM algorithm has considerable trouble while using Euclidean distance for segmenting images which are corrupted by noises and other imaging artifacts. The conventional FCM algorithm is independent of spatial information of pixels in the image, but the pixels in the image are highly correlated and the spatial relationship of neighboring pixels is an essential characteristic in image segmentation. This nature of FCM provides the noisy segmented results.[13–17] To overcome these drawbacks, many researchers have developed new modified FCM which is incorporated by the concepts such as kernel trick, additional term, penalty term, entropy term, and spatial neighborhood information terms. To increase the segmentation ability, Zhang and Chen[18] formulated kernel-based FCM with spatial constraint term (KFCM-S), which is based on the concept of kernel trick and neighborhoods of pixels. In Ref. 12, Siyal and Yu proposed modified FCM for automated segmentation of medical images to deal with the intensity inhomogeneities and Gaussian noise effectively. A modified FCM with spatial information was introduced in Ref. 13 to reduce the noisy elements in the dataset. A spatially constrained kernel clustering method was introduced in Ref. 19 to speed up the algorithms in clustering images. Yang and Tsai[20] introduced Gaussian kernel-based FCM algorithm (GKFCM) with a spatial bias correction to prevail over the shortcoming of computational time required and lack of enough robustness to noise and outliers. To improve the segmentation process, Zanaty *et al.*[21] proposed alternative Kernelized FCM algorithms (KFCM), which include the spatial information into the membership function of FCM. Kang *et al.*[22] developed an adaptive weighted averaging FCM (AWA-FCM) algorithm in which the spatial influence of the neighboring pixels on the central pixel is included in the segmentation process. To improve the smoothness toward piecewise-homogeneous segmentation and reduce the edge-blurring effect, Wang *et al.*[23] proposed adaptive spatial information-theoretic clustering (ASIC) algorithm, which is obtained by incorporating spatial constrains to FCM. To remove the bias field, Sikka *et al.*[24] introduced new modified FCM algorithm for medical image segmentation. Although the above algorithms provide good results in image segmentation, their performance depreciates promptly when the noise level is amplified. Usually the Gaussian function[25–27] is used as kernel trick in many modified KFCM algorithms. The computational cost is quite high for large datasets and fails to eradicate the heavy noises while using the Gaussian function.

To surmount these limitations, this paper proposes two effective KFCM[27–29] which incorporate the perception of tolerance vector[30–33] and entropy term[34–36] for segmenting the DCE-BMRIs. Further, this paper introduces a novel effective kernel function for the kernel trick of proposed algorithm. Addition of tolerance vector in each pixel of DCE-BMRI in the proposed algorithms for removing the pixel-level noises and smoothing the boundaries

between two tissue classes of breast MRI has been performed. Also, the incorporation of spatial neighborhood term in the proposed algorithm has been done to filter out noise and other image artifacts and reduce classification ambiguities. The new effective kernel function is employed to provoke a class of robust non-Euclidean distance measures for the original data space for deriving new objective functions and thus clustering the non-Euclidean structures in data. Besides, it augments the robustness of the original clustering algorithms to noise and outliers, and it decreases the computational complexity. The efficacy and robustness of the proposed algorithms are revealed through the experimental results on DCE-BMRI.

The remainder of this paper is structured as follows. In Sec. 2, we illustrate the notion of Kernelized and entropy-based FCM with tolerance. Subsequently, we propose a new robust spatially constrained kernelized FCM algorithms named as SKFCMT and SKFCMTER in Sec. 3. The experimental comparisons are presented in Sec. 4. Finally, Sec. 5 gives our conclusions.

2. Notion of Kernelized and Entropy-Based FCM with Tolerance

The objective function of FCM for partitioning a dataset $\{x_i\}_{i=1}^{n}$ into c clusters is given by

$$J_{fcm}(U,V)=\sum_{i=1}^{n}\sum_{k=1}^{c}u_{ik}^{m}d_{ik}^{2},$$

$$\text{where } d_{ik}=\|x_i-v_k\|, \tag{1}$$

where $V=\{v_k\}_{k=1}^{c}$ is the set of cluster centers and the array $U=[u_{ik}]_{n\times c}$ represents the partition matrix which is satisfying the following conditions

$$\sum_{k=1}^{c}u_{ik}=1,\quad 1\le i\le n\quad \text{where } 0\le u_{ik}\le 1 \tag{2}$$

$$0\le\sum_{i=1}^{n}u_{ik}\le n. \tag{3}$$

The parameter $m>1$ is the weighting exponent which controls the noise sensitivity and the level of the effect of membership grade in the computation of cluster centers. Most commonly the gray-level value or intensity feature of image pixel is used in image clustering. Thus, when high membership values are assigned to pixels whose intensities are close to the cluster center of its particular class, and low membership values are assigned whose intensities are far from the cluster center, the objective function of FCM is minimized by using Lagrangian multiplier's method.

In general, by minimizing the objective function, we can get the fuzzy membership functions u_{ik} and cluster centers v_k as follows:

$$u_{ik}=\frac{\left(\frac{1}{d^2(x_i,v_k)}\right)^{\frac{1}{m-1}}}{\sum_{j=1}^{c}\left(\frac{1}{d^2(x_i,v_j)}\right)^{\frac{1}{m-1}}}\quad\begin{matrix}i=1,2,\ldots,n\\ k=1,2,\ldots,c\end{matrix} \tag{4}$$

$$v_k=\frac{\sum_{i=1}^{n}u_{ik}^{m}x_i}{\sum_{i=1}^{n}u_{ik}^{m}}. \tag{5}$$

There exist image pixels in real images that are ambiguous and they cannot be classified consistently based on feature attribute(s) alone. Thus the tolerance vector is added with each pixel for getting consistent classification of the image pixels. Then we obtain the objective function of fuzzy c-means with tolerance (FCM-T) as follows:

$$J_{fcm\_t}(U,V,\tau)=\sum_{i=1}^{n}\sum_{k=1}^{c}u_{ik}^{m}\|x_i+\tau_i-v_k\|^2. \tag{6}$$

Subject to the constraint

$$\|\tau_i\|^2\le\kappa_i^2\quad(\kappa_i^2>0) \tag{7}$$

where κ_i is the maximum tolerance of τ_i and $\kappa_i\in R^{+}$.

The above notion can be minimized by Karush−Kuhn−Tucker (KKT)[32] method; by minimizing the Eq. (6) we obtain the following:

$$\text{Membership grade } u_{ik}=\frac{1}{\sum_{j=1}^{c}\left(\frac{\|x_i+\tau_i-v_k\|^2}{\|x_i+\tau_i-v_j\|^2}\right)^{\frac{1}{m-1}}}. \tag{8}$$

Updating equation for center is

$$v_k=U_k^{-1}\sum_{i=1}^{n}u_{ik}^{m}(x_i+\tau_i), \tag{9}$$

where $U_k=\sum_{i=1}^{n}u_{ik}^{m}$.

The tolerance vector is calculated by using

$$\tau_i=-\alpha_i\left(\sum_{k=1}^{c}u_{ik}(x_i-v_k)\right), \tag{10}$$

where

$$\alpha_i = \min\left\{\kappa_i\left\|\sum_{k=1}^{c} u_{ik}^m(x_i - v_k)\right\|^{-1}, \left(\sum_{k=1}^{c} u_{ik}^m\right)^{-1}\right\}.$$

In order to cluster nonlinear structured datasets of images, the kernel trick is introduced to FCM-T by replacing Euclidean distance in FCM-T. The notion of objective function of Kernelized Fuzzy c-Means with Tolerance (KFCM-T) is

$$J_{kfcm\_t}(U,V,\tau) = \sum_{i=1}^{n}\sum_{k=1}^{c} u_{ik}^m \|\varphi(x_i+\tau_i) - \varphi(v_k)\|^2. \tag{11}$$

Here

$$\|\varphi(x_i+\tau_i) - \varphi(v_k)\|^2 = \langle \varphi(x_i+\tau_i) - \varphi(v_k), \varphi(x_i+\tau_i) - \varphi(v_k)\rangle \tag{12}$$

and

$$\langle \varphi(x_i+\tau_i), \varphi(v_k)\rangle = G(x_i+\tau_i, v_k) \tag{13}$$

$$\|\varphi(x_i+\tau_i) - \varphi(v_k)\|^2 = G(x_i+\tau_i, x_i+\tau_i) + G(v_k,v_k) - 2G(x_i+\tau_i, v_k). \tag{14}$$

Since the Gaussian kernel $G(x_i+\tau_i, x_i+\tau_i) = 1$, the objective function of KFCM-T in Eq. (11) can be rewritten as

$$J_{kfcm\_t}(U,V,\tau) = 2\sum_{i=1}^{n}\sum_{k=1}^{c} u_{ik}^m[1 - G(x_i+\tau_i, v_k)]. \tag{15}$$

In a similar way to the standard FCM-T algorithm, the objective function in Eq. (15) is minimized under the constraint of U and τ. By using the KKT conditions for u_{ik}, v_k and τ_i, we obtain membership grade, updating cluster center and updating tolerance vector as follows:

$$u_{ik} = \frac{1}{\sum_{j=1}^{c}\left(\frac{[1-G(x_i+\tau_i,v_k)]}{[1-G(x_i+\tau_i,v_j)]}\right)^{\frac{1}{m-1}}}, \tag{16}$$

$$v_k^{(t)} = U_k^{-1}\sum_{i=1}^{n} u_{ik}^m G(x_i+\tau_i, v_k^{(t-1)})(x_i+\tau_i), \tag{17}$$

where $U_k = \sum_{i=1}^{n} u_{ik}^m G(x_i+\tau_i, v_k^{(t-1)})$ and t is the iteration count.

$$\tau_i = -\alpha_i\left(\sum_{k=1}^{c} u_{ik}^m(x_i - v_k^{(t-1)})\right), \tag{18}$$

where

$$\alpha_i = \min\left\{\kappa_i\left\|\sum_{k=1}^{c} u_{ik}^m G(x_i+\tau_i, v_k^{(t-1)})(x_i - v_k^{(t-1)})\right\|^{-1}, \left(\sum_{k=1}^{c} u_{ik}^m G(x_i+\tau_i, v_k^{(t-1)})\right)^{-1}\right\}.$$

To prevent the trivial solutions within the scope of KFCM-T and to control the cluster volume sizes, an entropy term is added with KFCM-T as additional term.

We introduce entropy term with L_{kfcm_t} as follows:

$$J_{ekfcm\_t}(U,V,\tau) = \sum_{i=1}^{n}\sum_{k=1}^{c} u_{ik} G(x_i+\tau_i, v_k^{(t-1)}) + \gamma^{-1}\sum_{i=1}^{n}\sum_{k=1}^{c} u_{ik}\log u_{ik}. \tag{19}$$

The objective function Eq. (19) is minimized iteratively and membership function, cluster center, and tolerance vector are obtained as follows:

$$u_{ik} = \left(\sum_{j=1}^{c}\exp(-\gamma G(x_i+\tau_i, v_j))\right)^{-1} \times \exp(-\gamma G(x_i+\tau_i, v_k)) \tag{20}$$

$$v_k^{(t)} = U_k^{-1}\sum_{i=1}^{n} u_{ik} G(x_i+\tau_i, v_k^{(t-1)})(x_i+\tau_i), \tag{21}$$

where

$$U_k = \sum_{i=1}^{n} u_{ik} G(x_i+\tau_i, v_k^{(t-1)})$$

$$\tau_i^{(t)} = -\alpha_i\left[\sum_{i=1}^{n} u_{ik} G(x_i+\tau_i^{(t-1)}, v_k^{(t-1)})(x_i - v_k^{(t-1)})\right], \tag{22}$$

where

$$\alpha_i = \min\left\{\kappa_i^2\left[\sum_{k=1}^{c} u_{ik} G(x_i+\tau_i, v_k^{(t-1)})\left\|x_i - v_k^{(t-1)}\right\|\right]^{-1}, \left[\sum_{k=1}^{c} u_{ik} G(x_i+\tau_i, v_k^{(t-1)})\right]^{-1}\right\}$$

The parameters γ, κ, and σ are adjustable by users.

3. Spatially Constraint KFCM Algorithms for Image Segmentation

Although the Standard FCM algorithm works well on most noise-free images, it has serious limitations: it does not incorporate any information about spatial context, which causes it to be sensitive to noise and imaging artifacts and it suffers from poor performance if the separation boundaries between tissues are nonlinear. Further Standard FCM fails to advance the similarity measurement of the pixel intensity and the center of clusters, since it has not taken into account the neighborhood magnetic fields.

To solve the problems, this section proposed an effective FCM to advance the similarity measurement of the pixel intensity and the center of clusters by considering neighborhood magnetism to segment the nonlinear boundaries between the tissues. This section develops the effective method for segmenting DCE-BMRIs based on the concept of kernel trick, tolerance, entropy term, and spatial penalty term. The entropy term will advance the similarity measurement of the pixel intensity and the center of clusters, and the penalty terms act as a regularizer to regularize the solution toward piecewise-homogeneous labeling. The main purpose of using the kernel tricks is to cluster the non-Euclidean structured pixel data by inducing a set of robust non-Euclidean distance measures for the original data space.

3.1. *Gaussian kernel function measure with new distance*

In recent years, a number of powerful kernel-based learning machines were used for solving the problem of nonlinear structured data. It has successfully been applied in the field of pattern recognition and image processing.

A nonlinear mapping of original data space into high-dimensional feature space S has been employed in the studies of kernel method for having nonlinear classification boundaries. The nonlinear mapping is defined as

$$\varphi : R^p \to S. \tag{23}$$

Here an object x is mapped into S and

$$\varphi(x) = (\varphi_1(x), \varphi_2(x), \ldots), \tag{24}$$

where $\varphi(x)$ may have the infinite dimension, even x is the p-dimensional vector. The kernel function can be expressed in terms of inner product of high-dimensional feature data as

$$G(x, y) = \langle \varphi(x), \varphi(y) \rangle. \tag{25}$$

The function $G(x, y)$ is known as kernel function and is defined as

$$G(x_i + \tau_i, v_k) = \exp\left(-\frac{d(x_i + \tau_i, v_k)}{\sigma^2} \right), \tag{26}$$

where σ is the adjustable parameters of the above kernel functions.

Generally, the usual Euclidean distance is used in Gaussian function. But in order to reduce the distortions in the pixels of images, we used Bray−Curtis distance instead of usual distance to measure Gaussian function. Bray−Curtis distance appears to have more utility than other distance measures and is given by

$$d(x_i + \tau_i, v_k) = \frac{\sum_{q=1}^{p} |x_{iq} + \tau_{iq} - v_{kq}|^2}{\sum_{q=1}^{p} |x_{iq} + \tau_{iq} + v_{kq}|^2}.$$

3.2. *Spatial constraint-based KFCM with tolerance*

This method is derived from the conventional FCM by incorporating the concept of tolerance vector, kernel function, and spatial penalty term. To obtain consistent classification of image pixels that are ambiguous, the tolerance vector is added with each pixel of images that are to be segmented. For avoiding poor accuracy in segmentation of images that are affected by noise, outliers, and other imaging artifacts, we modify the objective function of FCM-T by incorporating the spatial penalty term containing the neighborhood informations of each pixel. And, the kernel trick is introduced into proposed FCM-T in order to find the structure of nonlinear pixel data. The effective objective function for SKFCMT is given by

$$\begin{aligned} J_{\mathrm{SKFCMT}}(U, V, \tau) &= 2 \sum_{i=1}^{n} \sum_{k=1}^{c} u_{ik}^m [1 - G(x_i + \tau_i, v_k)] + \frac{2\eta}{N_R} \\ &\quad \times \sum_{i=1}^{n} \sum_{k=1}^{c} u_{ik}^m \sum_{r \in N_I} (1 - u_{rk})^m, \end{aligned} \tag{27}$$

where $(\eta = \bar{X}/c)$ and N_I stands for the set of neighboring pixels that exists in a window around

x_i (do not include x_i itself) and N_R is the cardinality of N_I; η controls the effect of the neighborhood penalty term for each pixel and to have desirable membership function for each pixel. In a similar way to FCM-T, Eq. (27) is solved by using the KKT method.

3.2.1. *Obtaining membership grade*

To find well-defined membership grade for every pixel, first we consider the KKT condition for u_{ik}. (i.e.) the condition $\frac{\partial J_{\text{SKFCMT}}}{\partial u_{ik}} = 0$, we get membership grade as

$$u_{ik} = \frac{1}{\sum_{j=1}^{c} \left(\frac{[1-G(x_i+\tau_i,v_k)]+\frac{2\eta}{N_R}\sum_{r\in N_I}(1-u_{rk})^m}{[1-G(x_i+\tau_i,v_j)]+\frac{2\eta}{N_R}\sum_{r\in N_I}(1-u_{rj})^m} \right)^{\frac{1}{m-1}}}. \tag{28}$$

The membership grade of each pixel to the cluster center is updated using Eq. (28), which represents the probability of ith pixel belonging to kth cluster. Because of adding the tolerance with each pixel and containing the neighborhood informations, this membership grade of pixel depends not only upon its own intensity but also on that of the nearest pixels of each pixel x_i. This approach diminishes the effect of heavy noise on an image pixel.

3.2.2. *Updating equation for cluster centers*

The updating equation of cluster center helps the algorithm to work well and converge the optimal solution with less iterations. The effective updating equation for cluster center is obtained by using KKT method.

Solving the minimization problem Eq. (27) for v_k, using the KKT condition $\frac{\partial J_{\text{SKFCMT}}}{\partial v_k} = 0$, we can get cluster center as

$$v_k^{(t)} = U_k^{-1}\left[\sum_{i=1}^{n} u_{ik}^m G(x_i+\tau_i, v_k^{(t-1)}) y(x_i+\tau_i, v_k^{(t-1)})(x_i+\tau_i)\right], \tag{29}$$

where

$$U_k = \sum_{i=1}^{n} u_{ik}^m G(x_i+\tau_i, v_k^{(t-1)}) y(x_i+\tau_i, v_k^{(t-1)}),$$

such that

$$y(x_i+\tau_i, v_k) = \frac{\sum_{s=1}^{p}\left(|x_{is}+\tau_{is}+v_{ks}^{(t-1)}|^2 + |x_{is}+\tau_{is}-v_{ks}^{(t-1)}|^2\right)}{\left(\sum_{s=1}^{p}|x_{is}+\tau_{is}+v_{ks}^{(t-1)}|^2\right)^2}.$$

These cluster centers quickly approach desired position in the final clusters. This allows the execution of algorithm in a robust manner.

3.2.3. *Obtaining value for tolerance*

The tolerance vector is used to get clear boundaries between tissues of breast image during the process of segmenting DCE-breast MRI. The tolerance vector value is obtained by solving the minimization problem of (27) using the KKT conditions for $\tau_i \frac{\partial J_{\text{SKFCMT}}}{\partial \tau_i} = 0$ and $\delta_i \frac{\partial J_{\text{SKFCMT}}}{\partial \delta_i} = 0$:

$$\tau_i^{(t)} = -\alpha_i \begin{bmatrix} x_i \sum_{k=1}^{c} u_{ik}^m G(x_i+\tau_i^{(t-1)}, v_k) \\ \quad \times y(x_i+\tau_i^{(t-1)}, v_k) \\ -\sum_{k=1}^{c} u_{ik}^m G(x_i+\tau_i^{(t-1)}, v_k) \\ \quad \times y'(x_i+\tau_i^{(t-1)}, v_k) v_k \end{bmatrix}, \tag{30}$$

where

$$\alpha_i = \min\left\{ \kappa_i^2 \left[\left\| \begin{matrix} x_i \sum_{k=1}^{c} u_{ik}^m G(x_i+\tau_i^{(t-1)}, v_k) \\ \quad \times y(x_i+\tau_i^{(t-1)}, v_k) \\ -\sum_{k=1}^{c} u_{ik}^m G(x_i+\tau_i^{(t-1)}, v_k) \\ \quad \times y'(x_i+\tau_i^{(t-1)}, v_k) v_k \end{matrix} \right\|^{-1} \right], \left[\begin{matrix} \sum_{k=1}^{c} u_{ik}^m G(x_i+\tau_i^{(t-1)}, v_k) \\ \quad \times y(x_i+\tau_i^{(t-1)}, v_k) \end{matrix} \right]^{-1} \right\}$$

where

$$y(x_i+\tau_i, v_k) = \frac{\sum_{s=1}^{p}(|x_{is}+\tau_{is}^{(t-1)}+v_{ks}|^2 + |x_{is}+\tau_{is}^{(t-1)}-v_{ks}|^2)}{(\sum_{s=1}^{p}|x_{is}+\tau_{is}^{(t-1)}+v_{ks}|^2)^2}$$

$$y'(x_i+\tau_i, v_k) = \frac{\sum_{s=1}^{p}(|x_{is}+\tau_{is}^{(t-1)}+v_{ks}|^2 - |x_{is}+\tau_{is}^{(t-1)}-v_{ks}|^2)}{(\sum_{s=1}^{p}|x_{is}+\tau_{is}^{(t-1)}+v_{ks}|^2)^2}.$$

The above minimization problem is summarized as follows.

3.2.4. *Algorithm for SKFCMT*

Step 1. Fix value for the number of cluster c, the maximum tolerance set κ for data X and m. Assign the initial values for τ and V.

Step 2. Evaluate membership grade by using Eq. (28).

Step 3. Update tolerance by using Eq. (30).

Step 4. Update cluster center by using Eq. (29).

Step 5. Verify the stopping criterion for $J(U, V, \tau)$. If the criterion is not satisfied, repeat Steps 2–4.

3.3. *Spatial constraint-based Kernel FCM with tolerant entropy regularized term*

In this subsection, we proposed the spatial constraints-based Kernel Fuzzy c-Means with Tolerant Entropy Regularized Term (SKFCMTER) for obtaining well segmentation technique to segment the DCE-breast MRIs. To improve the clustering effect, the entropy term has been added with the above algorithm. The entropy is considered as the special form of describing uncertainty of pixels. So it regularizes the process of clustering technique, especially in the case of pixel data with uncertainty. The incorporation of spatial constraint term into this proposed algorithm can filter the noise, outliers, and other imaging artifacts and reduce the classification vagueness. The proposed algorithm is obtained by minimizing the following objective function iteratively

$$\begin{aligned} &J_{\text{SKFCMTER}}(U, V, \tau) \\ &= 2\sum_{i=1}^{n}\sum_{i=1}^{c} u_{ik}[1 - G(x_i + \tau_i, v_k)] \\ &\quad + \frac{2\eta}{N_R}\sum_{i=1}^{n}\sum_{k=1}^{c} u_{ik}^{m}\sum_{r\in N_I}(1 - u_{rk})^m \\ &\quad + \gamma^{-1}\sum_{i=1}^{n}\sum_{k=1}^{c} u_{ik}\log u_{ik}. \end{aligned} \tag{31}$$

The constraint for membership grade and tolerance are same as the previous algorithms. In a similar way to FCM-T, Eq. (31) is solved by using the KKT method.

3.3.1. *Obtaining membership grade*

To obtain a membership grade for each pixel, first we consider the KKT zero-gradient condition for u_{ik} (i.e.) $\frac{\partial J_{\text{SKFCMTER}}}{\partial u_{ik}} = 0$. Then we get,

$$u_{ik} = \frac{1}{\sum_{j=1}^{c}\left(\frac{\exp\left(\gamma[1-G(x_i+\tau_i,v_k)]+\frac{2\eta}{N_R}\sum_{r\in N_I}(1-u_{rk})^m\right)}{\exp\left(\gamma[1-G(x_i+\tau_i,v_j)]+\frac{2\eta}{N_R}\sum_{r\in N_I}(1-u_{rj})^m\right)}\right)^{\frac{1}{m-1}}}. \tag{32}$$

The membership grade for assigning the pixel to concern cluster is calculated by Eq. (32).

3.3.2. *Updating equation for cluster centers*

The cluster centers are used to capture the structure of the data in each cluster. Generally, an accuracy of clustering result depends on the cluster center. We can obtain the effective updating equation for cluster center by minimizing Eq. (31) using the KKT condition $\frac{\partial J_{\text{SKFCMTER}}}{\partial v_k} = 0$. By solving the minimization problem for v_k, we get the cluster center as

$$v_k^{(t)} = U_k^{-1}\left[\sum_{i=1}^{n} u_{ik}G(x_i + \tau_i, v_k^{(t-1)}) \times y(x_i + \tau_i, v_k^{(t-1)})(x_i + \tau_i)\right], \tag{33}$$

where

$$U_k = \sum_{i=1}^{n} u_{ik}G(x_i + \tau_i, v_k^{(t-1)})y(x_i + \tau_i, v_k^{(t-1)}),$$

where

$$y(x_i + \tau_i, v_k^{(t-1)}) = \frac{\sum_{s=1}^{p}(|x_{is} + \tau_{is} + v_{sk}^{(t-1)}|^2 + |x_{is} + \tau_{is} - v_{ks}^{(t-1)}|^2)}{\left(\sum_{s=1}^{p}|x_{is} + \tau_{is} + v_{ks}^{(t-1)}|^2\right)^2},$$

where t is the iteration count.

The cluster center is updated by using Eq. (33). It is a robust workup of the clustering process. Further, it reduces the computational time and leads the algorithm to converge to the solution with less iteration.

3.3.3. *Obtaining value for tolerance*

The tolerance value is very important in the DCE-breast MR image segmentation to obtain clear boundaries between the tissues. The tolerant value is obtained by using the KKT condition for $\tau_i \frac{\partial J_{\text{SKFCMTER}}}{\partial \tau_i} = 0$ and $\delta_i \frac{\partial J_{\text{SKFCMTER}}}{\partial \delta_i} = 0$. By solving

these conditions, we can get,

$$\tau_i^{(t)} = -\alpha_i \left[x_i \sum_{k=1}^{c} u_{ik} G(x_i + \tau_i^{(t-1)}, v_k) y(x_i + \tau_i^{(t-1)}, v_k) - \sum_{k=1}^{c} u_{ik} G(x_i + \tau_i^{(t-1)}, v_k) y'(x_i + \tau_i^{(t-1)}, v_k) v_k \right], \tag{34}$$

where

$$\alpha_i = \min \left\{ \kappa_i^2 \left[\left\| x_i \sum_{k=1}^{c} u_{ik} G(x_i + \tau_i^{(t-1)}, v_k) \times y(x_i + \tau_i^{(t-1)}, v_k) - \sum_{k=1}^{c} u_{ik} G(x_i + \tau_i^{(t-1)}, v_k) \times y'(x_i + \tau_i^{(t-1)}, v_k) v_k \right\| \right]^{-1}, \left[\sum_{k=1}^{c} u_{ik} G(x_i + \tau_i^{(t-1)}, v_k) \times y(x_i + \tau_i^{(t-1)}, v_k) \right]^{-1} \right\}$$

where

$$y(x_i + \tau_i^{(t-1)}, v_k) = \frac{\sum_{s=1}^{p} (|x_{is} + \tau_{is}^{(t-1)} + v_{ks}|^2 + |x_{is} + \tau_{is}^{(t-1)} - v_{ks}|^2)}{(\sum_{s=1}^{p} |x_{is} + \tau_{is}^{(t-1)} + v_{ks}|^2)^2}$$

$$y'(x_i + \tau_i^{(t-1)}, v_k) = \frac{\sum_{s=1}^{p} (|x_{is} + \tau_{is}^{(t-1)} + v_{ks}|^2 - |x_{is} + \tau_{is}^{(t-1)} - v_{ks}|^2)}{(\sum_{s=1}^{p} |x_{is} + \tau_{is}^{(t-1)} + v_{ks}|^2)^2}.$$

From the above discussion, we obtain the following iterative algorithm.

3.3.4. *Algorithm for SKFCMTER*

Step 1. Fix value for the number of cluster c, the maximum tolerance set κ for data X and γ. Set the initial values of τ and V.

Step 2. Update membership grade by using Eq. (32).

Step 3. Update cluster center by using Eq. (33).

Step 4. Update tolerance by using Eq. (34).

Step 5. Verify the stopping criterion for $J(U, V, \tau)$. If the criterion is not satisfied, repeat Steps 2–4.

4. Experimental Study

In this section, we illustrate some experimental results to compare the segmentation performance of spatially constraints KFCM (KFCM-S), SKFCMT, and SKFCMTER. To show the performances of the three algorithms under noises on the real DCE-BMRIs, we apply the algorithms for segmenting left and right DCE-BMRI and proton density left and right ce-BMRIs given in Figs. 1(a), 1(b) and Figs. 2(a), 2(b), respectively. We test the performance of the algorithms when the images corrupted by "Gaussian" noises shown in Figs. 1(c), 1(d) and Figs. 2(c), 2(d). It is clear from Figs. 1, 2(e) and 2(f) KFCM-S has poor performance in the presence of Gaussian noise. From the Figs. 1 and 2(g)–2(j), it is clear that the proposed kernel versions with spatial constraints are superior to the corresponding classical algorithm. On the whole, our proposed algorithm achieves better segmentation results under Gaussian noise.

Table 1 lists the segmentation accuracy of the three algorithms on left and right DCE-BMRI noisy images, where segmentation accuracy is defined using silhouette value in Refs. 37 and 38.

The silhouette accuracy $s(i)$ of the object i is derived by the equation

$$s(i) = \frac{v(i) - w(i)}{\max\{v(i), w(i)\}}.$$

For each object, we denote by the cluster to which it belongs and compute

$$v(i) = \frac{1}{|G|} - 1 \sum_{j \in G, i \neq j} d(i, j).$$

The equation $v(i)$ is the average distance between the ith data and all other objects in the cluster G. Now consider a second cluster H different from G and put

$$d(i, H) = \frac{1}{|H|} \sum_{j \in H} d(i, j) = \text{average dissimilarity of: } i \text{ to all objects of } H \text{ and } H \neq G.$$

After computing $d(i, H)$ for all H, we take the smallest of those.

$$w(i) = \min_{H \neq G} d(i, H).$$

The cluster B which attains this minimum [that is $d(i, B) = w(i)$] is called the neighborhood of object i, this is the second best cluster for object i.

These silhouette average values measures the clustering strength in the clustering assignment of a particular observation, with well-clustered observations having values near 1 and poorly clustered observations having values near −1.

From Table 1, the best clustering validities 0.77 and 0.78 were obtained for our SKFCMTER during the experimental work on DCE-breast Magnetic Resonance Images. Further, it is clear from Figs. 1 and 2(g)−2(j) that our proposed segmentation algorithms succeeded well in correcting and classifying the breast data and the algorithms almost completely eliminate the effect of noise in images. The clustering algorithms presented in this study are advantageous in that it should be robust to cluster more general-shaped datasets.

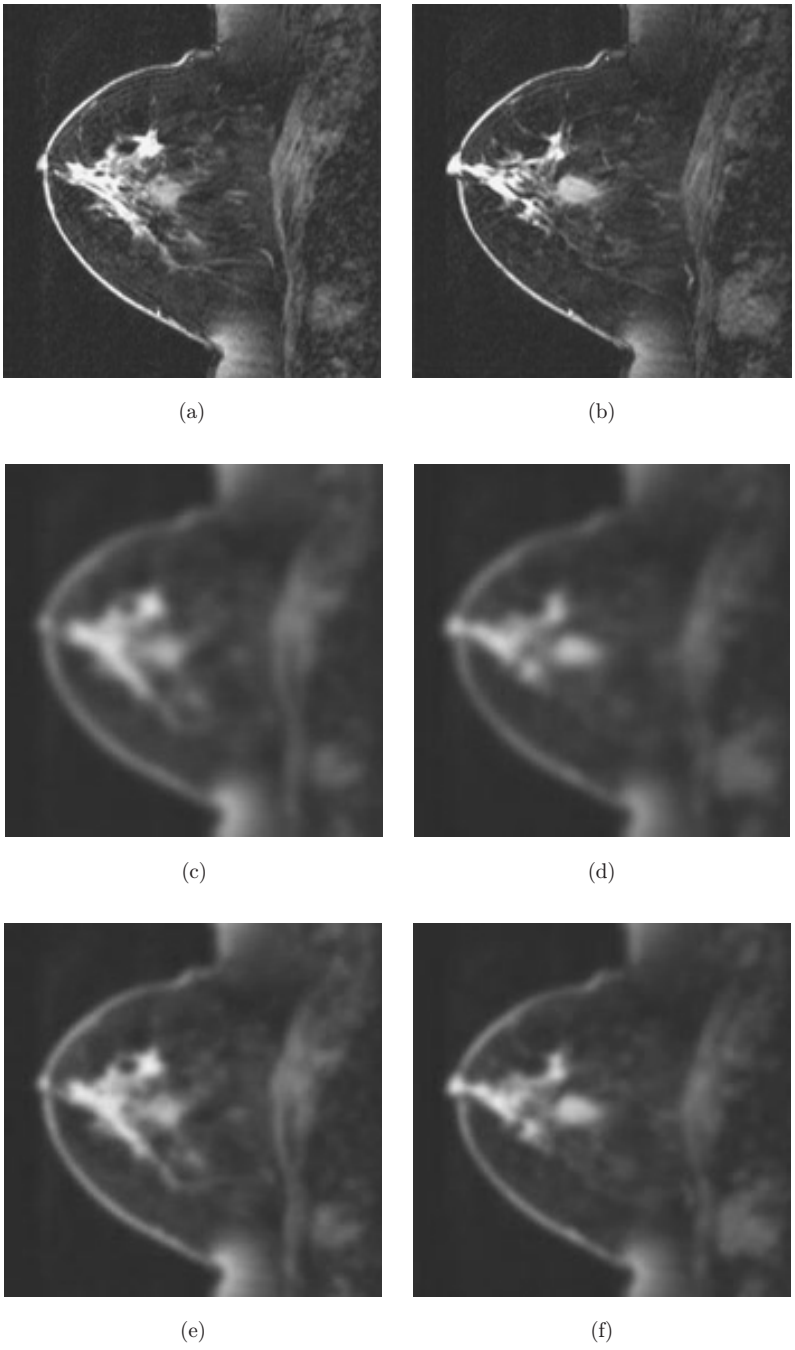

Fig. 1. Segmentation results. (a, b) DCE-left and right BMRI. (c, d) Corrupted by Gaussian noise. (e, f) Segmentation result by KFCM-S. (g, h) Segmentation result by SKFCMT. (i, j) Segmentation result by SKFCMTER.

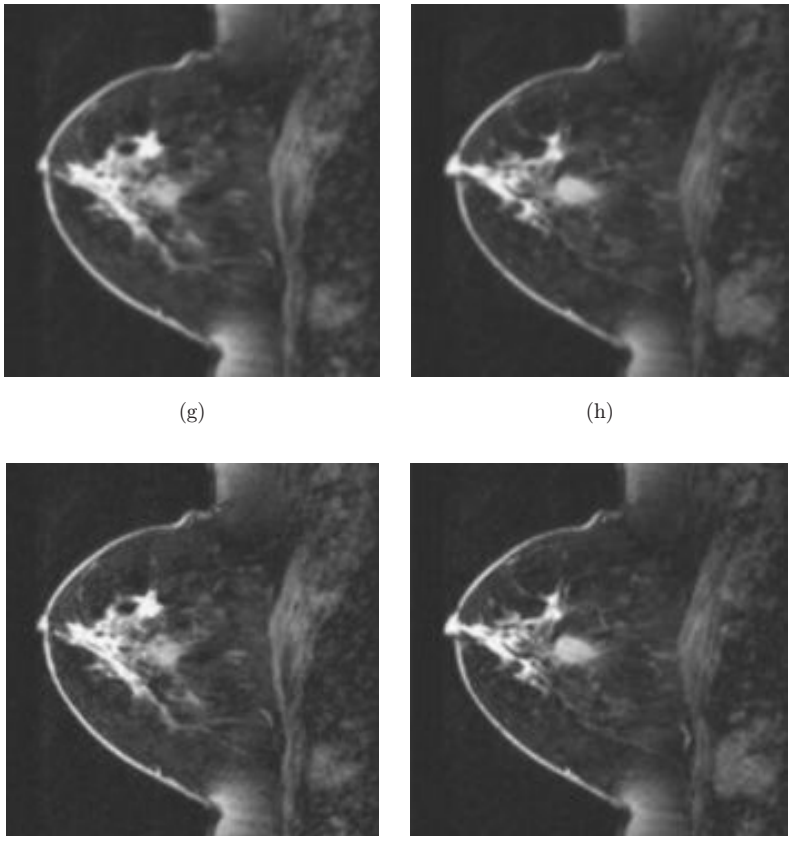

(g) (h)

(i) (j)

Fig. 1. (*Continued*)

4.1. *Performance of proposed methods in computational time*

To show the effective of proposed methods in reducing the computational time for running the algorithm this subsection describes the experimental results on artificial image which is generated by random data given in Figs. 3(a) and 3(b).

Our first experiment introduces the Standard FCM algorithm to an artificial image which is generated by random data. The image with 14 objects includes two classes with intensity values taken from 1 and 14. We test the algorithms' performance when the given image in Fig. 3(b) is corrupted by improper order. Figure 4(a) gives the segmentation result of

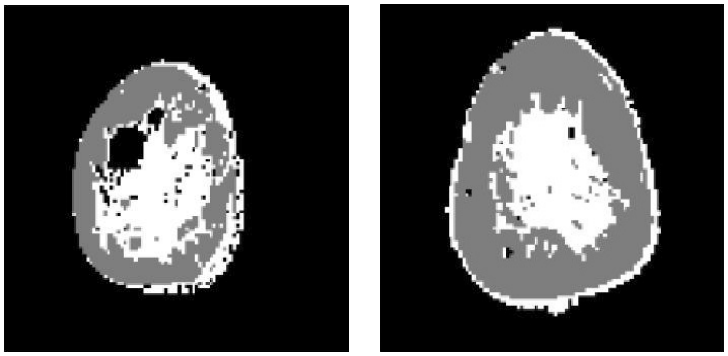

(a) (b)

Fig. 2. Segmentation results. (a, b) ce-left pd-BMRI and right pd-BMRI. (c, d) Corrupted by Gaussian noise. (e, f) Segmentation result by KFCM-S. (g, h) Segmentation result by SKFCMT. (i, j) Segmentation result by SKFCMTER.

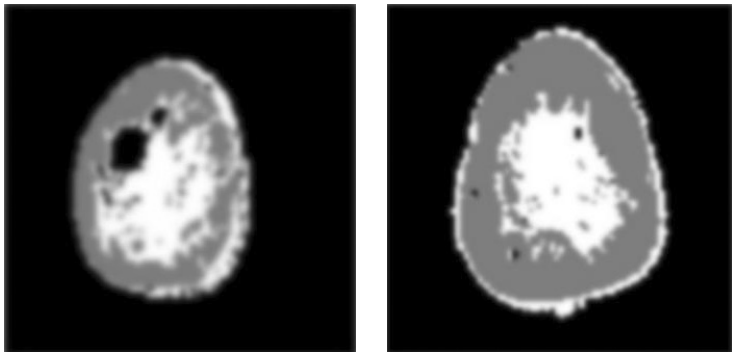

(c) (d)

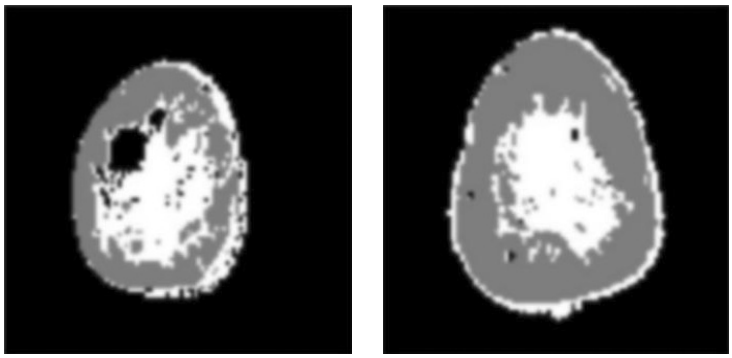

(e) (f)

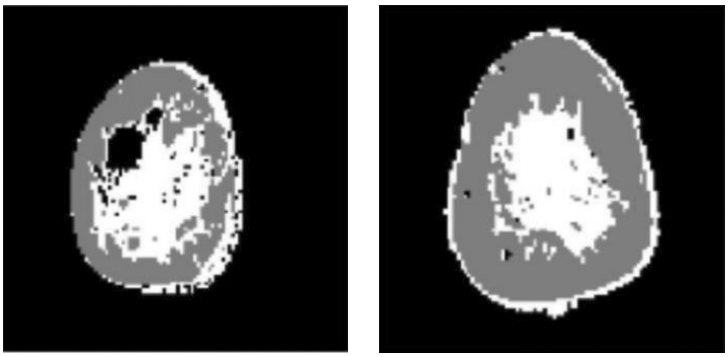

(g) (h)

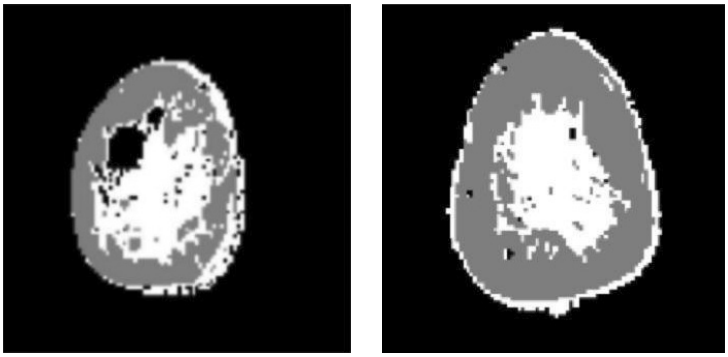

(i) (j)

Fig. 2. (*Continued*)

Table 1. Segmentation accuracies.

Name of algorithms	No. of clusters	Silhouette value of DCE-BMRI	Accuracy of DCE-BMRI (%)	Silhouette value of pd-ce-BMRI	Accuracy of ce-BMRI (%)
KFCM-S	4	0.50	50	0.54	54
SKFCMT	4	0.75	75	0.76	76
SKFCMTER	4	0.77	77	0.78	78

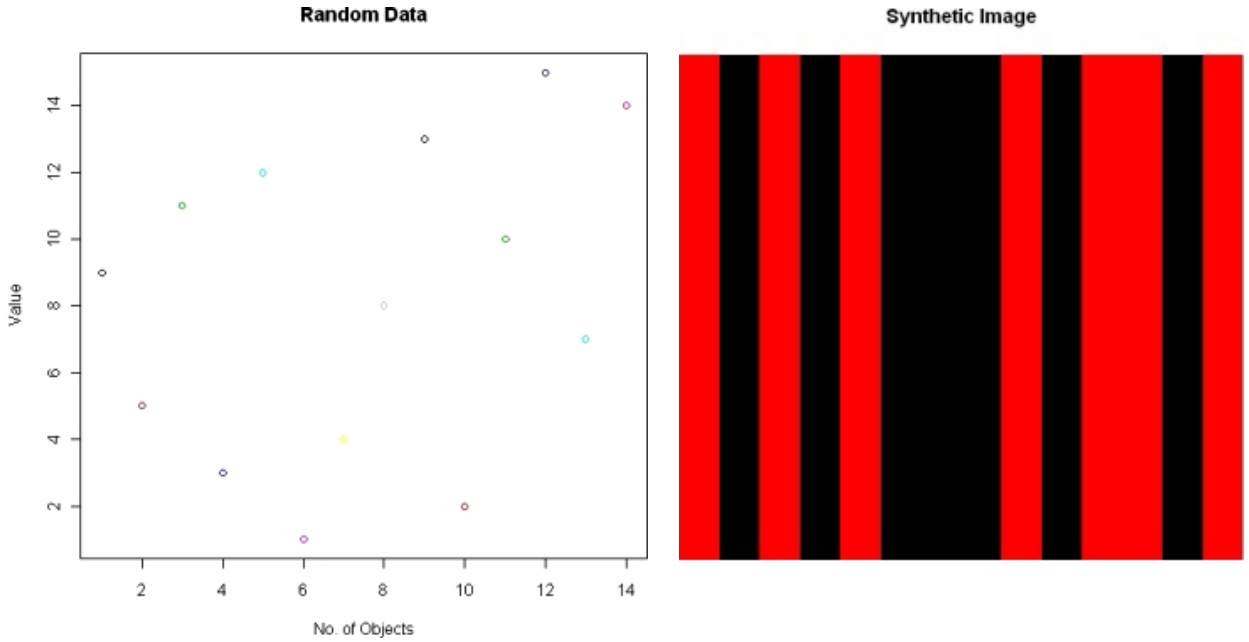

(a) (b)

Fig. 3. (a) Random data. (b) Corrupted image.

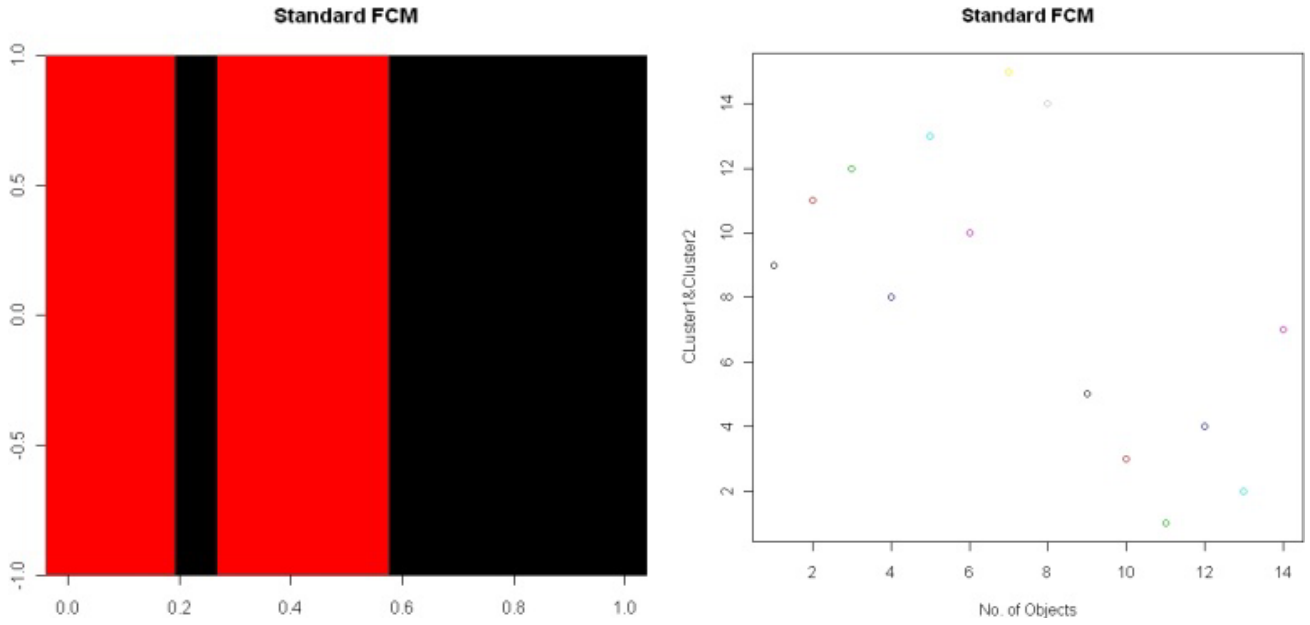

(a) (b)

Fig. 4. (a) Image by Standard FCM. (b) Clusters by Standard FCM.

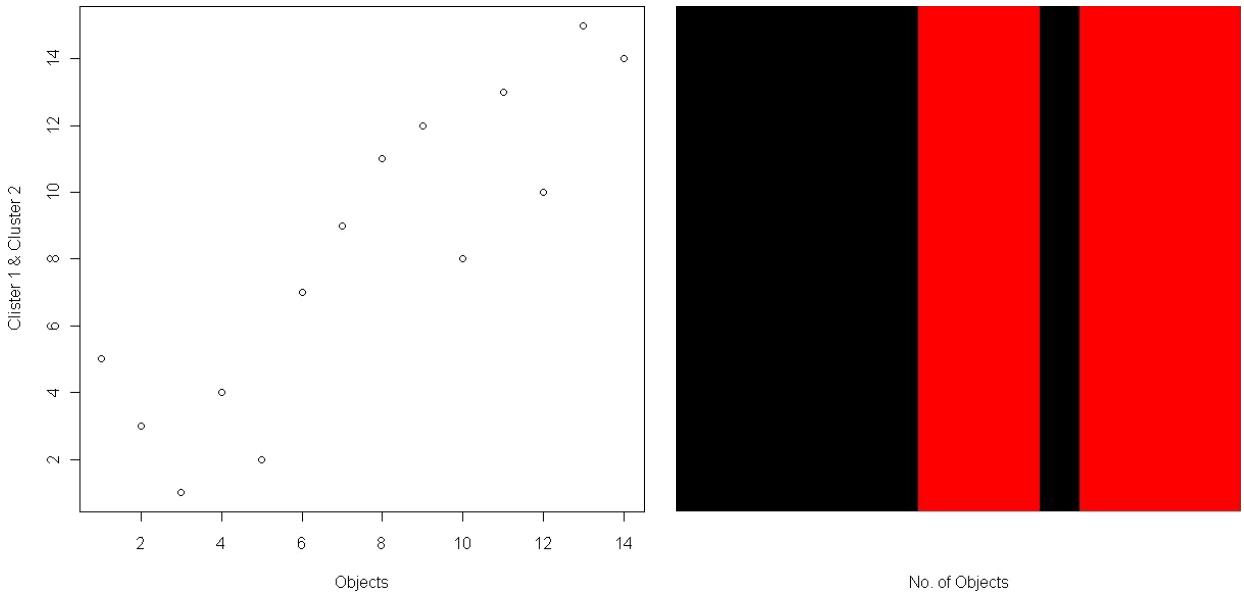

(a) (b)

Fig. 5. (a) Clusters by SKFCMT. (b) Image by SKFCMT.

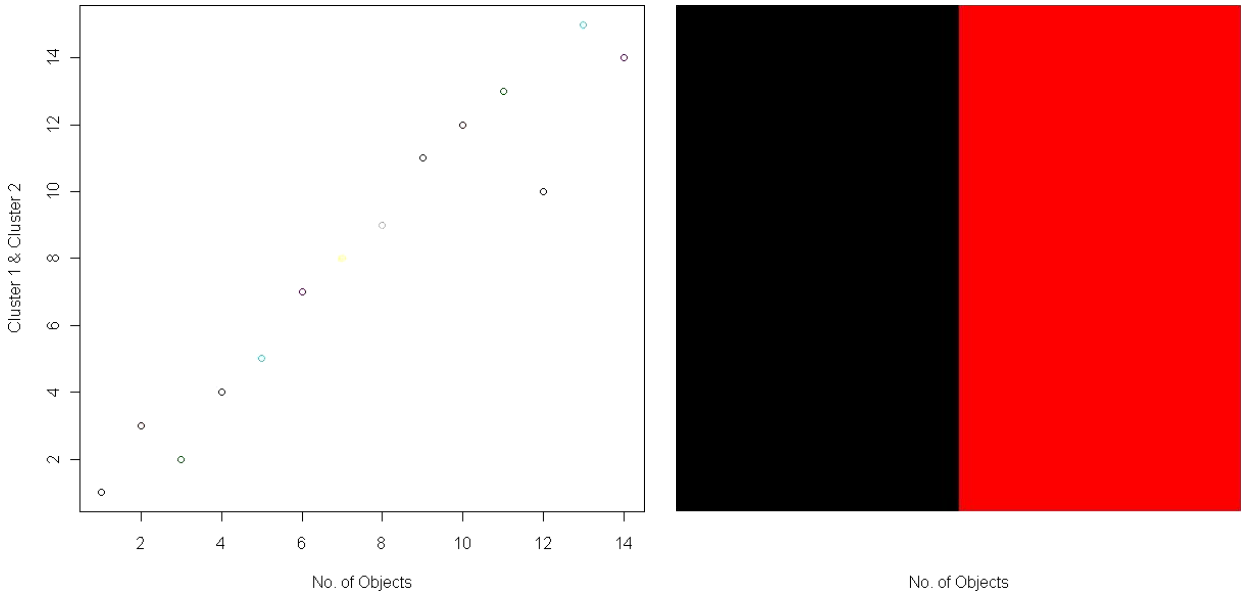

(a) (b)

Fig. 6. (a) Clusters by SKFCMTER. (b) Image by SKFCMTER.

Standard FCM. The Standard FCM takes 20 iterations to obtain the resulted clusters.

Now we introduce our proposed method SKFCMT to an artificial image to test its effect on performance. We set the initial cluster centers as 3.5 and 11.5. Figures 5(a) and 5(b) show the results of proposed SKFCMT under the improperly ordered different values of synthetic image. It is observed from Fig. 5(b) that the proposed SKFCMT FCM reduces the misclassification in colors and achieves

Table 2. Comparison of iteration count.

	No. of iterations	No. of clusters
Standard FCM	20	2
Proposed SKFCMT	9	2
Proposed SKFCMTER	8	2

better results than Standard FCM. The algorithm obtains the results after seven iterations of the algorithm.

Now we take proposed method SKFCMTER for implementing it to synthetic image. To test its effect on performance, we have initialized two cluster centers as 3.5 and 11.5 and divided the synthetic image into two partitions. Figures 6(a) and 6(b) show the results of proposed SKFCMTER. From Fig. 6(b), the numbers of misclassified objects reduced much and there are no improperly ordered colors on image. It can also be seen from Fig. 6(b) that the proposed method is superior to the corresponding proposed method SKFCMTER. According to Figs. 5(b) and 6(b), we know that under experimental approach of synthetic image, the proposed SKFCMT and SKFCMTER still achieve much better performance than the Standard FCM.

Table 2 shows the comparison of the number of iterations in the experiment of Standard FCM and proposed methods on synthetic image. The number of prototypes or centers was set as two. The Standard FCM takes 20 iterations to complete the experimental work on synthetic image for clustering it into two partitions. From Table 2, it is clear that our proposed methods achieve results with much less iterations than the Standard FCM. It is clear from our above observation that the proposed methods need less runtime to complete the experimental work.

5. Conclusions

In this paper, novel robust segmentation algorithms based on conventional FCM for image clustering were introduced. The proposed algorithms can detect the clusters of an image by overcoming the noise sensitiveness and other imaging artifacts of known FCM clustering algorithms and their variants. This was obtained by modifying the objective function in the traditional KFCM algorithm using concepts such as tolerant vector, entropy term, neighborhood attraction of each pixels, and a spatial penalty on the membership functions. The modified kernel-induced distance measure aims to guarantee the robustness both to noise and outliers. The efficacy of the proposed segmentation algorithms was tested through experimental study on real DCE-BMRIs and artificial images. The segmentation accuracy of the proposed segmentation algorithms was validated by using silhouette cluster validity. The results of this paper have shown that the proposed algorithms have more robustness to noises, outliers, and other artifacts than other existing algorithms. Particularly, the proposed method SKFCMTER acquired accurate segmentation result while balancing through between the noise and image details and concurrently enhancing the clustering performance among the other methods. And this effort, we hope that the proposed SKFCMTER algorithm is a capable technique for improving the efficiency of segmentation in DCE-BMR images.

Acknowledgment

This work was supported by DG CSIR (Ref. No.: 39-35/2010(SR)), India.

References

1. E. Vidholm, A. Mehnert, E. Bengtsson, M. Wildermoth, K. McMahon, S. Wilson, S. Crozier, "Hardware accelerated visualization of parametrically mapped dynamic breast MRI data," *Proc. MICCAI Workshop*: *Interaction in Medical Image Analysis and Visualization*, pp. 33−40 (2007).
2. J. P. Brockway, K. R. Subramanian, W. B. Carruthers, E. K. Insko, "Detection and visualization of inflammatory breast lesions using dynamic contrast enhanced MRI," *J. Magnetic Res. Imag.* (2004).
3. G. S. Karczmar, G. M. Newstead, M. Medved, A. M. Wood, H. Abe, F. I. Olopade, "High resolution MR breast imaging," *Medicamundi* **53**(1), 20−24 (2009).
4. H. D. Cheng *et al.*, "Colour image segmentation: Advances and prospects," *Pattern Recogn.* **34**, 2259−2281 (2001).
5. S. K. Fu, J. K. Mui, "A survey on image segmentation," *Pattern Recogn.* **13**, 3−16 (1981).
6. N. Pal, S. Pal, "A review on image segmentation techniques," *Pattern Recogn.* **26**, 1277−1294 (1993).
7. D. L. Pham, C. Y. Xu, J. L. Prince, "A survey of current methods in medical image segmentation," *Ann. Rev. Biomed. Eng.* **2**, 315−337 (2000).

8. L. Clarke *et al.*, "MRI segmentation: Methods and applications," *Magn. Reson. Imag.* **13**, 343−368 (1995).
9. Y. Hamasuna *et al.*, "Two clustering algorithms for data with tolerance based on Hard *c*-Means," *IEEE International Conference on Fuzzy Systems* (*FUZZIEEE2007*), pp. 688−691 (2007).
10. Y. Hamasuna *et al.*, "On hard clustering for data with tolerance," *J. Japan Soc. Fuzzy Theory and Intelligent Informatics*, **20**(3), 388−398 (2008).
11. Z. Hou *et al.*, "Regularized fuzzy c-means method for brain tissue clustering," *Pattern Recogn. Lett.* **28**, 1788−1794 (2007).
12. M. Y. Siyal, L. Yu, "An intelligent modified fuzzy c-means−based algorithm for bias estimation and segmentation of brain MRI," *Pattern. Recogn. Lett.* **26**, 2052−2062 (2005).
13. K. S. Chuang *et al.*, "Fuzzy c-means clustering with spatial information for image segmentation," *Comput. Med. Imag. Graphics* **30**, 9−15 (2006).
14. W. Chen, M. L. Giger, U. Bick, "A fuzzy c-means (FCM)-based approach for computerized segmentation of breast lesions in dynamic contrast-enhanced MR images," *Acad. Radiol.* **13**, 63−72 (2006).
15. F. Masulli, A. Schenone, "A fuzzy clustering-based segmentation system as support to diagnosis in medical imaging," *Artif. Intell. Med.* **16**(2), 129−147 (1999).
16. D. L. Pham, "Fuzzy clustering with spatial constraints," *Proc. IEEE International Conference on Image Processing*, New York, USA (2002).
17. W. M. Wells *et al.*, "Adaptive segmentation of MRI data," *IEEE Trans. Med. Imag.* **15**, 429−442 (1996).
18. D. Q. Zhang, S. C. Chen, "A novel kernelized fuzzy c-means algorithm with application in medical image segmentation," *Artifi. Intell. Med.* **32**, 37−50 (2004).
19. L. Liao, T. Lin, B. Li, "MRI brain image segmentation and bias field correction based on fast spatially constrained kernel clustering approach," *Pattern Recogn. Lett.* **29**, 1580−1588 (2008).
20. M. S. Yang, H. S. Tsai, "A Gaussian kernel-based fuzzy c-means algorithm with a spatial bias correction," *Pattern Recogn. Lett.* **29**, 1713−1725 (2008).
21. E. A. Zanaty, S. Aljahdali, N. Debnath, "A kernelized fuzzy c-means algorithm for automatic magnetic resonance image segmentation," *J. Comp. Met. Sci. Eng.* **9**, S123−S136 (2009).
22. J. Kang *et al.*, "Novel modified fuzzy c-means algorithm with applications," *Digital. Signal Proc.* **19**, 309−319 (2009).
23. Z. M. Wang *et al.*, "Adaptive spatial information-theoretic clustering for image segmentation," *Pattern Recogn.* **42**, 2029−2044 (2009).
24. K. Sikka *et al.*, "A fully automated algorithm under modified FCM framework for improved brain MR image segmentation," *Magn. Res. Imag.* **27**, 994−1004 (2009).
25. S. Miyamoto, D. Suizu, "Fuzzy c-means clustering using transformations into high-dimensional spaces," *Proc. 1st International Conference on Fuzzy Systems and Knowledge Discovery* **2**, 656−660 (2002).
26. D. Q. Zhang *et al.*, "Kernel-based fuzzy clustering incorporating spatial constraints for image segmentation," *IEEE Proc. Second International Conference on Machine Learning and Cybernetics*, Xi'an, China, 2−5 November (2003).
27. D. Q. Zhang, S. C. Chen, "Clustering incomplete data using kernel-based fuzzy c-means algorithm," *Neural Proc. Lett.* **18**(3), 155−162 (2003).
28. D. Q. Zhang, S. C. Chen, "Fuzzy clustering using kernel methods," *Proc. International Conference on Control and Automation*, Xiamen, China, June (2002).
29. D. Q. Zhang, S. C. Chen, "Robust image segmentation using FCM with spatial constraints based on new kernel-induced distance measure," *IEEE Transactions on Systems, Man and Cybernetics, Part B — Cybernetics* **34**(4), 1907−1916 (2004).
30. Y. Endo *et al.*, "Fuzzy c-means for data with tolerance," *Proc. 2005 International Symposium on Nonlinear Theory and Its Applications* (*NOLTA2005*), pp. 345−348 (2005).
31. Y. Hamasuna, Y. Endo, M. Yamashiro, "Fuzzy c-means clustering for data with tolerance using kernel functions," *IEEE Int. Conference on Fuzzy Systems*, July 16−21, pp. 744−750 (2006).
32. Y. Hamasuna, Y. Endo, S. Miyamoto, "On tolerant fuzzy c-means," *J. Adv. Comput. Intell. Intell. Inform.* (*JACIII*) **13**(4), 421−428 (2009).
33. R. Murata *et al.*, "On fuzzy c-means for data with tolerance," *J. Adv. Comput. Intell. Intell. Inform.* **10**(5), 673−681 (2006).
34. H. Ichihashi, K. Honda, N. Tani, "Gaussian mixture PDF approximation and fuzzy c-means clustering with entropy regularization," *Proc. 4th Asian Fuzzy System Symposium*, pp. 217−221 (2000).
35. R. P. Li, M. Mukaidono, "Gaussian clustering method based on maximum-fuzzy-entropy interpretation," *Fuzzy Sets and Systems* **102**, 253−258 (1999).
36. S. Miyamoto, M. Mukaidono, "Fuzzy c-means as regularization and maximum entropy approach," *Proc. 7th International Fuzzy Systems Association*

World Congress (*IFSA'97*), Vol. 2, Prague, 86−92 (1997).

37. J. Dermoudy, B.-H. Kang, D. Bhattacharyya, S.-H. Jeon, A. Farkhod, "Process of extracting uncover patterns from data: A review," *Int. J. Database Theory Appl.* **2**(2), 17−33 (2009).
38. V. P. Shah, N. H. Younan, S. S. Durbha, R. L. King, "Data transformation for primitive feature extraction in image information mining: A comparative study," *Workshop Proc. ESA-EUSC 2006*: *Image Information Mining for Security and Intelligence*, Spain, November (2006).